Supplementary Information for

A Fully Unsupervised Compartment-on-Demand Platform for Precise Nanolitre Assays of Time-Dependent Steady-State Enzyme Kinetics and Inhibition

Fabrice Gielen,[1] Liisa van Vliet,[1] Bartosz T. Koprowski,[3] Sean R. A. Devenish,[1] Martin Fischlechner,[1,5] Joshua B. Edel,[2] Xize Niu,[4,5] Andrew J. deMello[3*] and Florian Hollfelder[1*]*

[1] Department of Biochemistry, University of Cambridge, 80 Tennis Court Road, CB2 1GA, UK

[2] Department of Chemistry, Imperial College London, South Kensington, London, SW7 2AZ, UK

[3] Institute for Chemical and Bioengineering, Department of Chemistry and Applied Biosciences, ETH Zürich, Wolfgang-Pauli-Strasse 10, CH-8093, Zürich, Switzerland

[4] Faculty of Engineering and the Environment, University of Southampton, Southampton, SO17 1BJ, UK

[5] Institute for Life Sciences, University of Southampton, Southampton SO17 1BJ, UK

I. Design of the compartment-on-demand platform

A carousel made of polyether ether ketone (PEEK) holds a stainless steel ring on its top bearing equally spaced holes able to fit PCR tubes (100 µL volume; Molecular BioProducts). The tube bottoms were removed with a sharp scalpel to leave a hole with a diameter of 2 mm. The 42 mm stepper-motor (RS) was controlled *via* a control board (Phidgets Inc), which allowed rotational precision of 0.9 °. A miniature monostable solenoid 6V (DC) electromagnet (RS) with a stroke reaching around 5 mm in 50 ms moved a metallic arm on which a stainless steel hook was attached. The internal diameter of the hook was 500 µm. In a typical experiment, the PCR tubes were filled with 40 µL of sample. The PTFE tubing (ID 200 µm) was inserted inside the hook and came out vertically with a height of 4 mm above the hook as represented schematically in Figure S1.

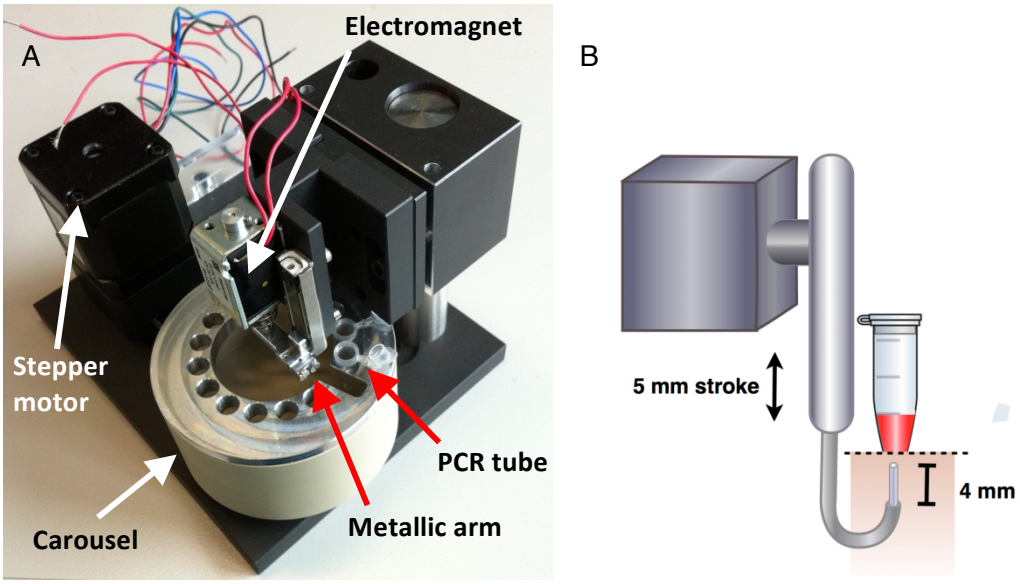

Figure S1. (A) Photograph of the droplet-generating robot. (B) Schematic of the hook attached to the solenoid providing the vertical motion. The hook contains the tubing that protrudes by 4 mm.

A custom-written Labview program commands both the stepper motor and the solenoid up and down motion. The stepper-motor was programmed to align the hook below the 15 sample locations. The solenoid was alternatively energized for a specified amount of time to provide the up and down motion. The adjustable variables for the program were the well location, the spatial ratio of the electromagnet (time 'up' divided by total time) and the frequency of 'up' and 'down' motions.

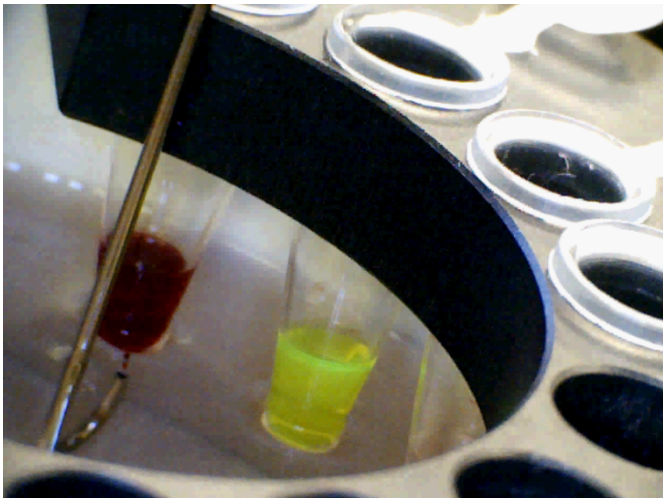

Figure S2. Still image from the video "Droplet_Generation" (available online as a video file as part of the SI). The samples are phenol red (10 mM, left), fluorescein (10 mM, middle) and PBS buffer (partly obscured on the right).

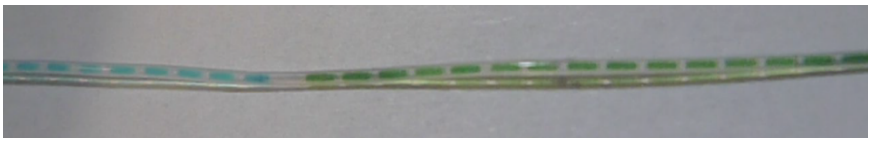

Figure S3. Still image from the video "Droplet_Sequence" (available online as a video file as part of the SI) that shows a sequence of droplets from various samples (distinguished by various different food dyes) in PTFE tubing (200 µm).

II. Droplet size is a function of suction flow rate and retention time in the aqueous phase and can be adjusted at will

The relationship between theoretical volume input and observed volume was tested by creating droplets of increasing sizes only changing the spatial ratio of the electromagnet from 10% to 100%. The frequency of droplet formation was 0.2, 1, 1 and 1.5 Hz for flow rates of 1, 3, 5 and 7 µL/min respectively.

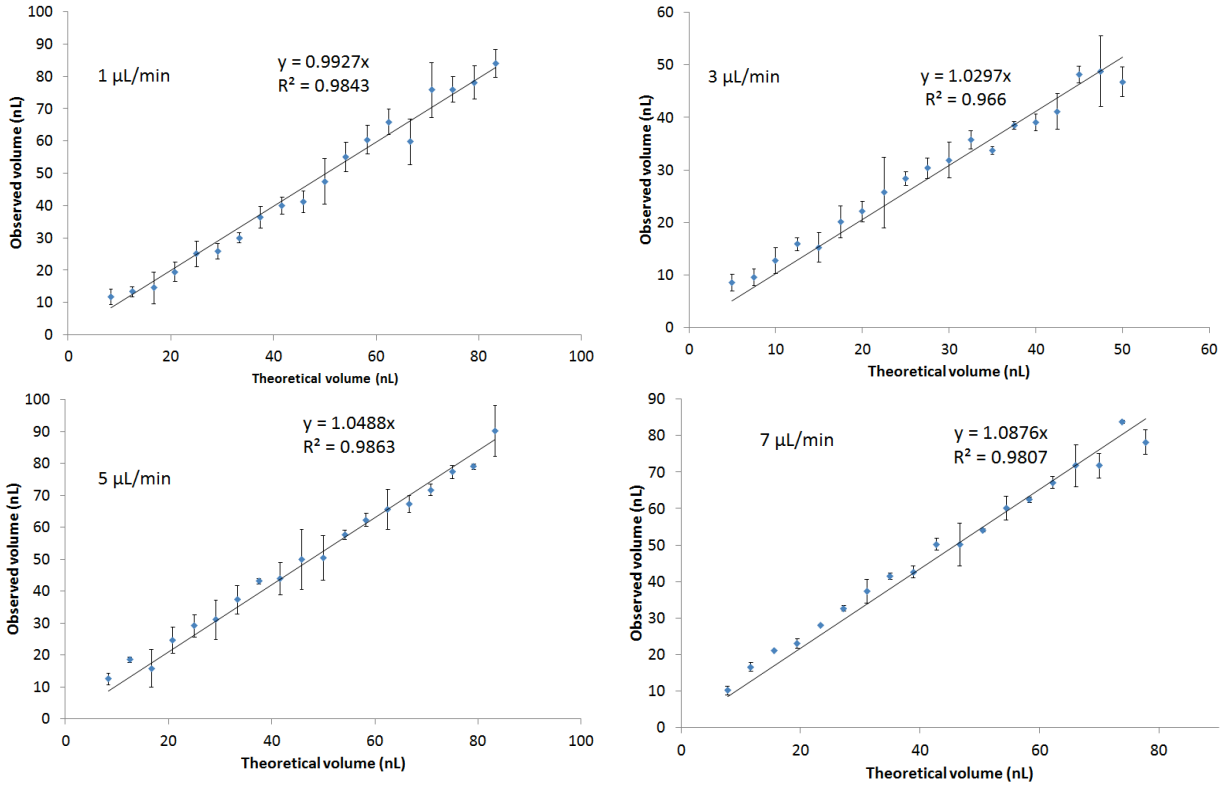

Figure S4. *Size calibration at different suction rates.* The linear correlation (r = 0.966 – 0.986) between droplet volume and retention time in the aqueous phase shows the technical robustness of the oil-to-aqueous transition.

The relationship between theoretical volumes and observed volumes is linear with slopes very close to 1. Deviations from linearity averaged 10% relative standard deviations. This may be due to the influence of pulsation caused by the syringe pump, which results in oscillating droplet sizes around the theoretical value. To compensate for the small deviations in droplet volumes, the lengths (and thus volumes) of droplets were systematically measured before running assays.

III. Droplet fusion in the tubing

A. Visualization

To visualize droplet catch-up and fusion, a movie was recorded at 30 fps of a small 10 nL droplet (2 mM phenol red in water) followed by a larger droplet (100 nL). The flow rate for droplet generation was 10 nL/s. The droplet pair was stopped and acceleration of the flow rate from zero to 25 µL/min was applied. In Figure S5, the acceleration was applied from left to right. The movie was subsequently processed using ImageJ. The intensity along a section of the tubing was recorded for all frames. The resulting plot is shown in Figure S5.

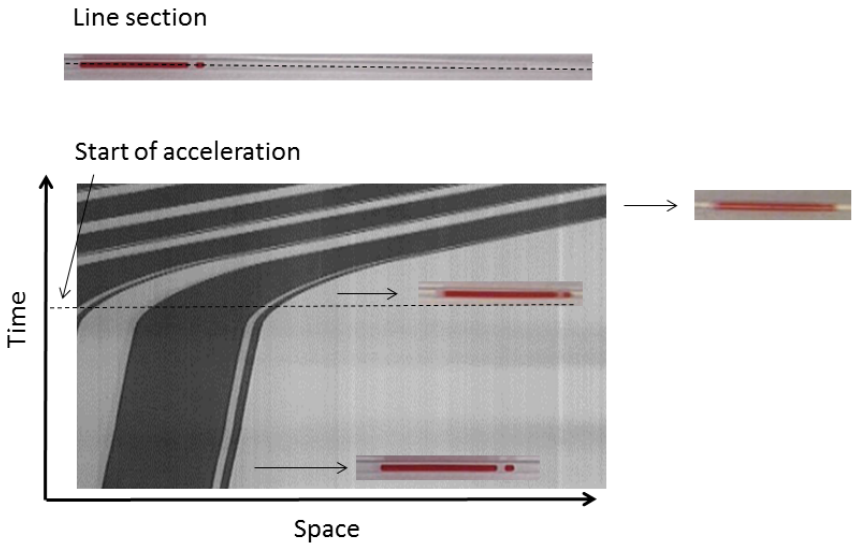

Figure S5. *Visual representation of droplet catch-up*. The x axis represents space while the y axis represents time.

The plot highlights that the clear gap between the small and larger droplets gets smaller as a function of time and eventually disappears.

B. Quantification of the success rate of droplet fusion

Droplets of various sizes were measured to travel at the same speed when separated by large oil gaps. However, when placed in close proximity, oil depletion between the two droplets started occurring with maximum effect taking place when a large droplet followed a smaller one or when the second droplet had a higher viscosity.

Fusion of 50 pairs of aqueous droplets containing phenol (1 mM) red was attempted and the merging success was measured as a function of suction rate. The number of successfully fused pairs was measured after a 15 cm distance. The acceleration applied was constant from 0 to 25 µL/min. It was found that merging was most successful when droplets were formed at low flow rates, with the merging success rate declining as droplets were formed more quickly. The success rate reaches as high as 90% with only droplets of roughly equal volume not catching up after the acceleration distance. Most of these droplets were found not to catch up even on distances over 80 cm.

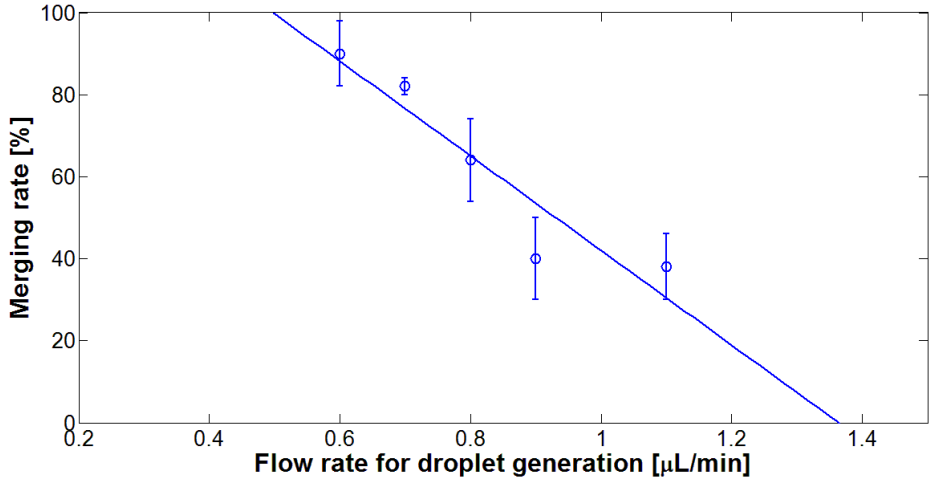

Figure S6. *Merging rate as a function of flow rate*. The merging rate increases with decreasing inter-droplet distances.

IV. Mixing of droplet contents after hydrodynamic merging of two droplets in round tubing

Content mixing after droplet fusion was studied by merging a small water droplet containing phenol red (1 mM) with a much larger aqueous buffer. Convection of the phenol red can be seen by tracking of the fusion event with a camera at 30 frames per second. Snapshots of the merging process are displayed in Figure S7.

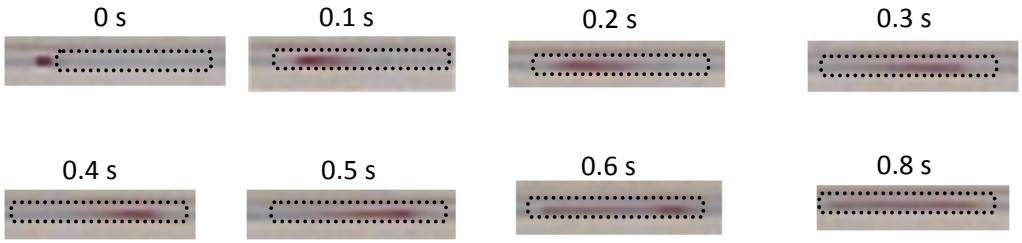

Figure S7. *Merging of a small droplet (containing 2 mM phenol red) with a long droplet (containing PBS).* Edges of the buffer droplet at the beginning of the experiment (time = 0 s) and the subsequent droplet fusion are outlined with a dotted line to aid visualisation for the buffer droplet initially and for the merged droplets afterwards. Convection flows within the merged droplet are seen with the fast displacement of the phenol red solution towards the back of the drop.

Complex mixing patterns form until a uniform distribution is reached after 3 to 5 seconds. As the timescale for this adjustment is much smaller than the timescale of the kinetics (typically recorded over 10 minutes, with time points every 20 sec), the mixing time can be neglected when analysing the reaction kinetics.

V. Automated gradient generation

The control program of the robot was modified to allow input of pairs with linearly varying sizes. Specifically, the volume of the first droplet was increased while the volume of the second decreased, so that the sum of the volumes of the two droplets remained constant. Merging of droplets with size ratios close to 1:1 was unreliable because oil leaked equally from the front and the rear droplet. To tackle this issue, a margin factor M was introduced to preserve a size difference between front and rear droplets. As the Labview program allows control of the frequency at which droplets are generated, the input frequency f_{1i} for the first droplet at pair *i* of *N* pairs was calculated from a fixed start frequency f_{start} and final frequency f_{end}. The equation for the frequency of generation of the front droplet f_{1i} was calculated as follows:

$$f_{1_i} = \left(\frac{1}{f_{end}} + \frac{\left(\frac{1}{f_{start}} - \frac{1}{f_{end}} \right) * (i-1)}{2 * \left(1 + \frac{M}{100} \right) * (N-1)} \right)^{-1}$$

For the rear droplet, the equation was:

$$f_{2_i} = \left(\frac{1}{f_{start}} - \frac{\left(\frac{1}{f_{start}} - \frac{1}{f_{end}} \right) * (i-1)}{2 * \left(1 + \frac{M}{100} \right) * (N-1)} \right)^{-1}$$

The program was tested for merging 50 phenol red (2mM)/water droplet pairs covering a range of size ratios such that the proportion of phenol red varied from 96.6% to 50%. The absorbance of these 50 merged pairs is shown in Figure S6. Here, the LED source used was cold white (Thorlabs).

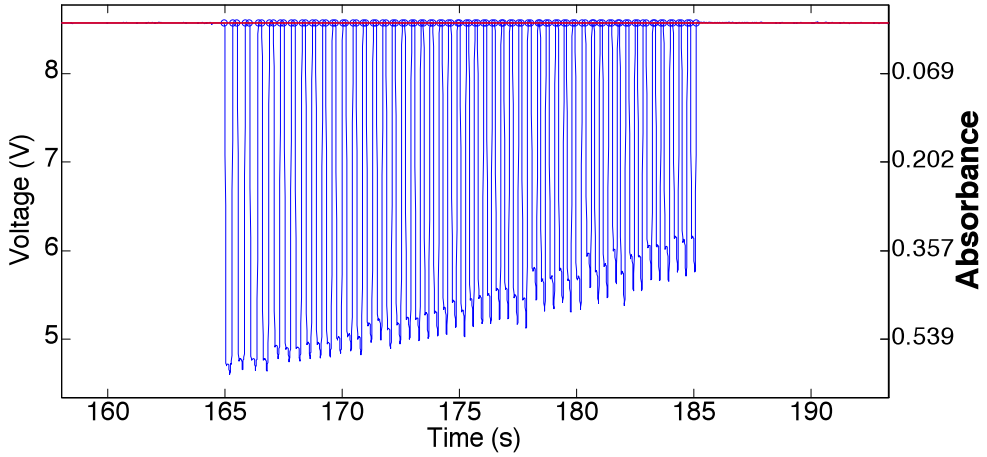

Figure S8. After merging phenol red (2 mM) and buffer in droplets of varying sizes, a linear gradient is created from high to low concentration of phenol red (2 mM down to 1 mM). The red line indicates the oil baseline.

In addition to size difference, it was found that more viscous droplets (for instance with mM amounts of substrate) tended to catch up with smaller and less viscous droplets in a faster manner and even over the 1:1 size ratio.

VI. Back and forth measurements

Droplets were moved back and forth by automatically reversing the flow, in response to detection of two droplets of high concentration (1 mM 4-nitrophenol) that were placed at the start and the end of the droplet sequences. A typical absorbance reading is shown in Figure S9, where a droplet sequence is read four times. The flow direction is indicated by black arrows. We refer to the alternation of their direction corresponds as a 'back-and-forth pattern'.

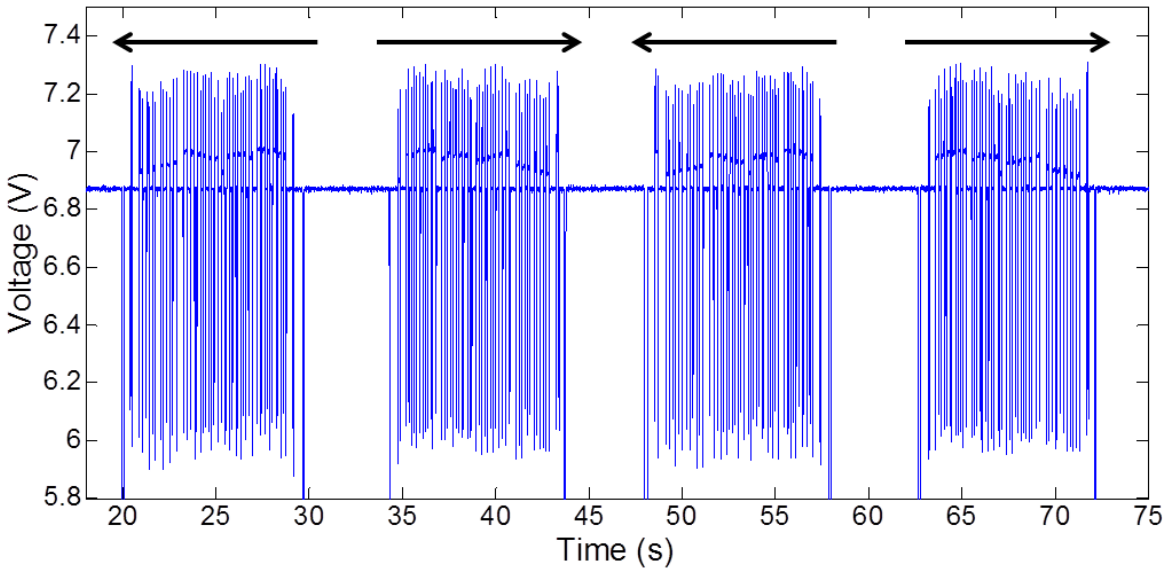

Figure S9. *Reading of a droplet sequence over time by reversing flow direction iteratively.* The voltage corresponds to the raw signal detected by the photo-detector and is used to quantify absorbance units.

VII. Background reaction

Control droplets containing only substrate in buffer at different concentrations were generated at the end of every kinetic sequence. The readings from these droplets were found to have a slope which is consistent with a self-hydrolysis process. Figure S10 shows the initial rates obtained for 5 droplets of substrate.

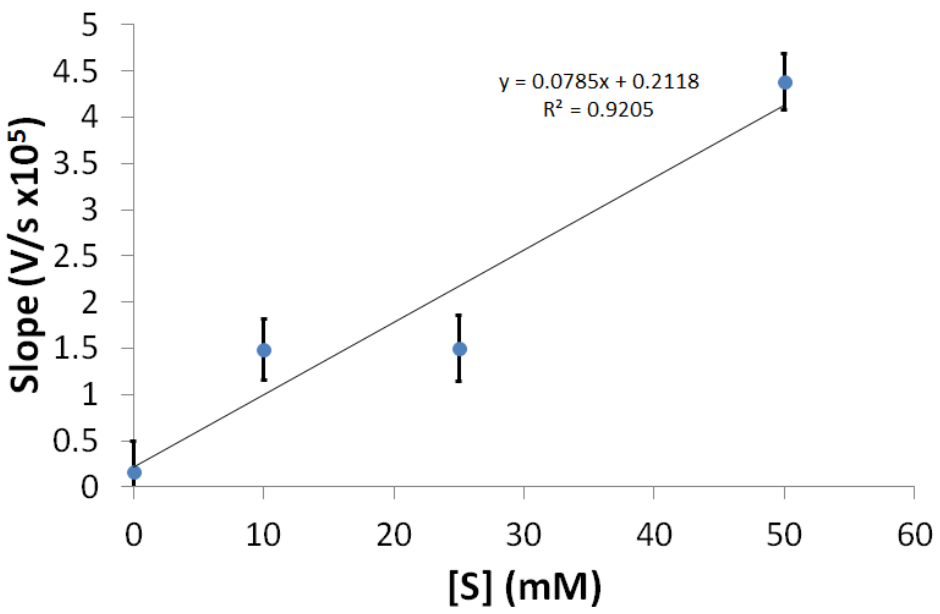

Figure S10. *Initial rates measured in droplets containing 4-nitrophenol glucopyranoside substrate in PBS buffer at pH 7.4.* Each point was an average of 5 droplets of volume 75 nL.

Performing the same control without introducing any enzymes in clean tubing and with a fresh oil bath resulted in similar results indicating this product formation is not linked with residual enzyme contamination. These initial rates represented typically 10-20% of the rates found in the catalyzed reaction. Therefore a correction factor proportional to substrate concentration was applied to each enzyme-substrate mix to correct for the observed hydrolysis. This phenomenon possibly occurs at the interface between carrier and aqueous phase.

VIII. Comparison with microtiter plate readings

Steady-state kinetics were performed with β-glucosidase from sweet almonds at 78 nM. The enzyme concentration was calculated so that the reaction would be linear over a timescale of 10 minutes while generating enough signal to produce quantitative plots from microdroplets.

Kinetic absorbance measurements were carried out in a SpectraMax Plus spectrophotometer (Molecular Devices). The Michaelis-Menten data for hydrolysis of 4-nitrophenyl glucopyranoside by β-glucosidase was measured to validate the microdroplet-generated data. In a 96-well plate, 100 µL reactions were carried out consisting of constant enzyme concentration (78 nM) and substrate concentration ranging between 0 and 40 mM. Rates were measured in triplicate at room temperature (21 °C) and initial rates plotted in Figure S11.

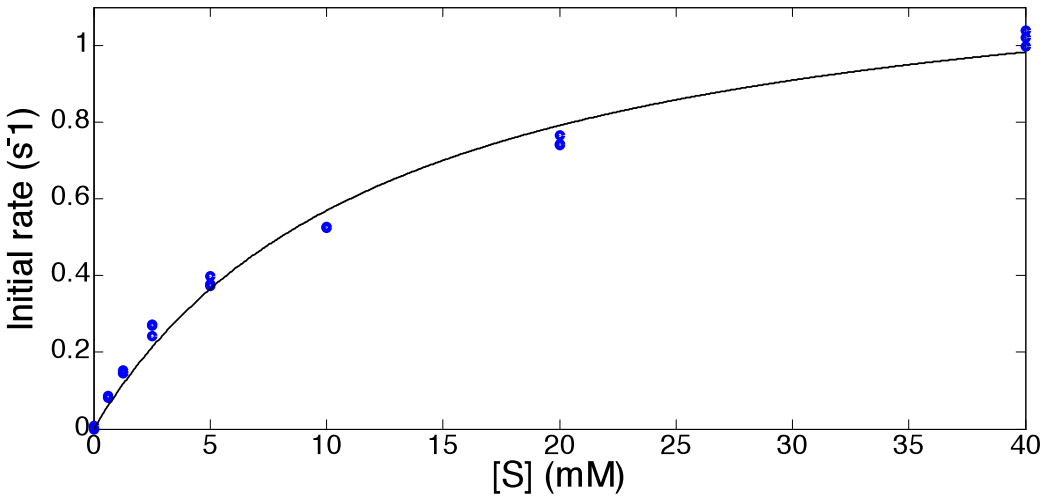

Figure S11. *A Michaelis-Menten plot for the hydrolysis of 4-nitrophenyl glucopyranoside catalysed by β-glucosidase as detailed in text. The Michaelis-Menten parameters of the fit were* $K_M = 12.8 \pm 4$ *mM and* $k_{cat} = 1.29 \pm 0.3$ s^{-1}.

Inhibition by 1-deoxynojirimycin hydrochloride (DNM) and conduriol B epoxide (CBE) was carried out at fixed enzyme and substrate concentrations (78 nM and 30 mM, respectively). The structures of both inhibiting compounds are shown in Figure S11 and normalized initial rate decreases are plotted versus inhibitor concentration in Figure S12.

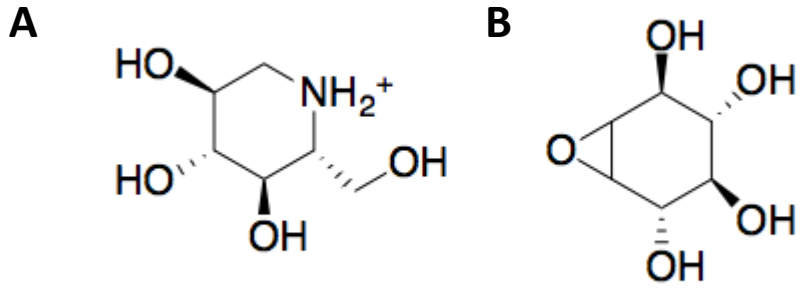

Figure S12. Structures of 1-deoxynojirimycin hydrochloride (A) and conduritol B epoxide (B).

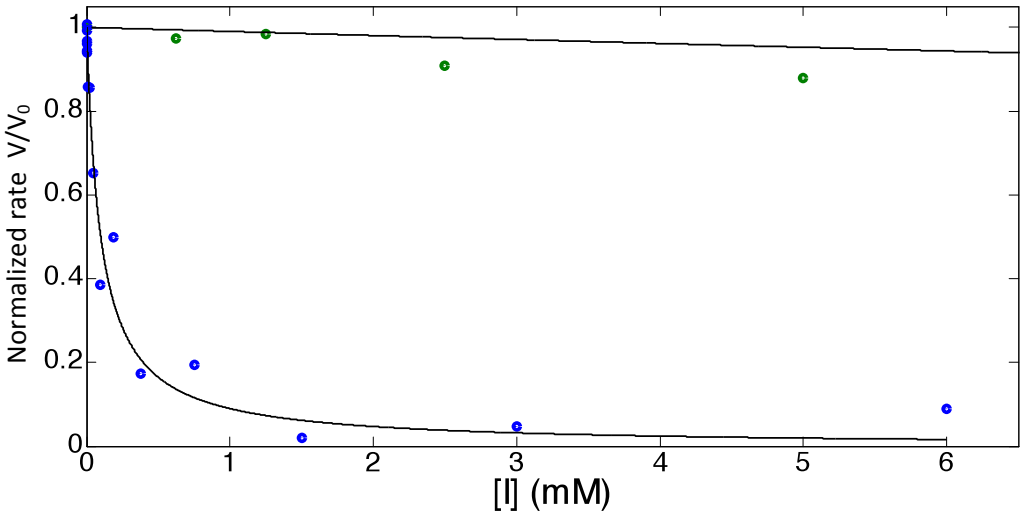

Figure S13. *Inhibition curves for DNM and CBE carried out in a microtiter plate.* The fit used for DNM had the functional form $\frac{V}{V_0} = \frac{1}{1+\frac{[I]}{IC_{50}}}$ while a line drawn for the CBE is merely to guide the eye.

The fit for DNM gave an IC_{50}=100 ± 30 µM translating into a mean K_I value of 30 µM. The literature value for K_I is 47 µM.